THE BELL SYSTEM TECHNICAL JOURNAL

DEVOTED TO THE SCIENTIFIC AND ENGINEERING ASPECTS OF ELECTRICAL COMMUNICATION

Volume 56 March 1977 Number 3

Thick Dielectric Grating on Asymmetric Slab Waveguide

By D. MARCUSE

(Manuscript received September 13, 1976)

We discuss an approximate theory of scattering losses of a guided mode in an asymmetric slab waveguide with a thick grating on one side. The theory is an extension of an exact theory of thick dielectric gratings published previously. The results of the theory are presented in graphical form. The coupling coefficient between two guided waves traveling in opposite directions is calculated and compared to perturbation theory.

I. INTRODUCTION

Diffraction gratings deposited on top of a thin-film waveguide are useful as input and output couplers.[1,2] A guided wave traveling in the thin-film waveguide is scattered out into the two regions (air and substrate) adjacent to the film as it encounters the region of the diffraction grating. Ordinarily, the power that is scattered out of the thin-film guide splits up into several grating lobes; the number and strength of these lobes depends on the grating period D, the depth of the grating $2a$, and on the shape of its teeth, as shown in Fig. 1. The relationship between the propagation constant β of the guided wave, the index of refraction n_i of the medium into which the grating lobe escapes at angle θ_{mi}, and the grating period length D is expressed by the following equation,[2]

$$\cos \theta_{mi} = \frac{\beta - (2\pi m/D)}{n_i k}. \tag{1}$$

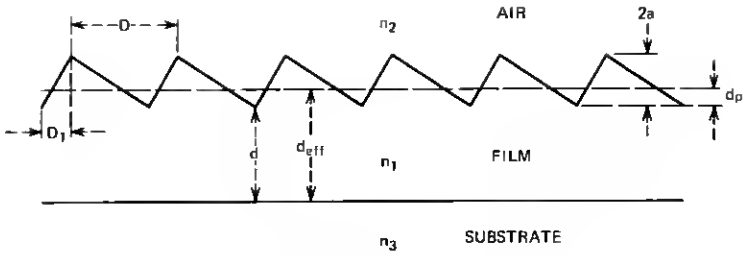

Fig. 1—Thick grating on a thin-film guide.

The integer m indicates the order of the grating lobe, $m = 1$ is the lobe of first order, $m = 2$, the lobe of second order, etc., and $k = 2\pi/\lambda$ is the free-space propagation constant. As the magnitude of the right-hand side of this equation exceeds the value unity, the scattering angle becomes imaginary and there is no scattered wave. (The angle θ_{mi} is measured with respect to the surface of the thin-film guide.) Thus, it is apparent that no scattered wave can escape from the film into medium i if $D < 2\pi/(\beta + n_i k)$. For values of D that are just larger than the right-hand side of the inequality (with n_i indicating the larger of the two refractive indices of the media adjacent to the film, the substrate say) a single grating lobe is radiated into the substrate. If D violates the inequality, with n_i being the refractive index of the air space (the region of lowest refractive index), a grating lobe is radiated into that region. If we let the value of D increase further, higher-order grating lobes begin to appear.

For purposes of coupling power from the outside into the film guide, a laser beam is directed at the grating and is aligned to coincide as closely as possible with one of the grating lobes.[2] If only one grating lobe exists, it is possible to capture most of the laser power and have it trapped in the thin-film guide. However, if other grating lobes exist, the laser power is split between the guided wave in the film and the other grating lobes so that the coupling efficiency for excitation of the trapped modes is reduced. It may be inconvenient to design a grating with only one lobe since this requires a grating with a very short period and also necessitates excitation of the thin-film guide through the substrate. For this reason, it is desirable to be able to control the amount of power radiated into undesirable grating lobes by shaping the form of the grating, that is, its teeth, in an appropriate way. Gratings with specially shaped teeth are known as blazed gratings.[3] An analysis of blazed gratings cannot be performed by using first-order perturbation theory because the grating, to be effective, must be thicker than is compatible with perturbation theory.

This paper proposes a new method of calculating grating responses

by an approximate method that, nevertheless, allows us to compute the response of thick gratings without having to search for the complex roots of a large determinant. Our approach is based on the exact grating theory described in Ref. 1. This exact theory is limited to TE waves (not an inherent limitation but one of convenience) and is applied to a grating defined as the boundary between two dielectric half spaces. A plane wave is incident from one side. The electromagnetic field outside of the grating is described as a superposition of infinitely many plane waves, most of which have propagation constants with one imaginary component. The field in the grating region is expressed as a double Fourier series. The unknown expansion coefficients are determined by matching of boundary conditions, not along the grating surface but along hypothetical planes adjacent to the grating.

This approach can easily be extended to the description of a grating on one side of a thin-film guide simply by adding the thin film to the structure and postulating plane waves in the film region. However, there is an important difference between the simple-grating and the waveguide-grating problems. The scattering problem of the grating between two half spaces is completely determined by the incident wave so that the amplitude coefficients of all the other waves can be obtained from an inhomogeneous equation system. The waveguide grating problem, on the other hand, leads to a homogeneous equation system. The distinction occurs because it is no longer possible to specify the direction of the incident wave, which is now the upward (or downward) traveling part of the standing wave pattern of the guided mode whose propagation constant is not known. In fact, the complex propagation constant would now be obtained as the solution of a determinantal eigenvalue equation.[2] However, the search for the complex solutions of a large determinantal equation is costly and time consuming and offsets the advantage of the original grating calculation.

To circumvent this problem, we propose a different approach. It is true that the exact eigenvalue of the determinantal equation is complex, but we know *a priori* that the real part of this complex solution, the propagation constant, is far larger than the imaginary part, the loss coefficient. This observation gives us confidence that it should be possible to determine the loss coefficient by computing the amount of radiated power once the problem has been approximately solved. The real part of the complex eigenvalue can be obtained by an approximation that is based on results obtained from the simpler grating theory described in Ref. 1. We have shown that the effective plane of reflection of the incident plane wave can be computed approximately by means of the WKB method. The comparison of the effective penetration depth computed from the WKB approximation with the exact result showed that the agreement was reasonable. We found that the penetration depth of the

wave was approximately given by the formula[1]

$$d_0 = \frac{4a\kappa_0^2}{3(n_1^2 - n_2^2)k^2} - \frac{1}{\kappa_0}\left[\frac{\pi}{4} - \arctan\frac{\gamma_0}{\kappa_0}\right]. \tag{2}$$

We use the definition

$$\kappa_0^2 = n_1^2 k^2 - \beta^2 \tag{3}$$

and

$$\gamma_0^2 = \beta^2 - n_2^2 k^2. \tag{4}$$

Figure 1 shows that $2a$ is the depth of the grating, n_1 the refractive index of the thin film, and n_2 represents the index of the medium above the film. The WKB solution that led to (2) fails (in the form used by us) as the grating becomes too thin. For this reason, we use as the penetration depth (see Figs. 12 and 13 of Ref. 1)

$$d_p = \begin{cases} d_0 \text{ if } d_0 < a \\ a \text{ if } d_0 > a \end{cases}. \tag{5}$$

The information gathered from Ref. 1 thus allows us to define an effective film thickness d_{eff} (see Fig. 1) as

$$d_{\text{eff}} = d + d_p \tag{6}$$

and thus enables us to calculate iteratively the propagation constant β from (3), (4), and[4]

$$\kappa_0 d_{\text{eff}} = \nu\pi + \arctan\frac{\gamma_0}{\kappa_0} + \arctan\frac{\delta_0}{\kappa_0}, \tag{7}$$

with

$$\delta_0^2 = \beta^2 - n_3^2 k^2 \tag{8}$$

(ν is the mode number of the guided wave; $\nu = 0$ for the lowest order TE mode.) The refractive index n_3 is the index of the medium on the other side of the film opposite the medium with index n_2.

Once the propagation constant of the guided mode is approximately known, we fix the value of that component of the standing wave inside of the thin film that approaches the grating and we solve the inhomogeneous equation system that results. It is clear that this equation system cannot provide an exact solution since we have already frozen the value of the propagation constant and have specified one of the two amplitudes associated with the guided wave to the right-hand side of the equation system, changing a homogeneous to an inhomogeneous equation system. However, we have checked tbat our approach gives precisely the same results as first-order perturbation theory for small values of the grating depth $2a$. Furthermore, the results obtained from this approximation

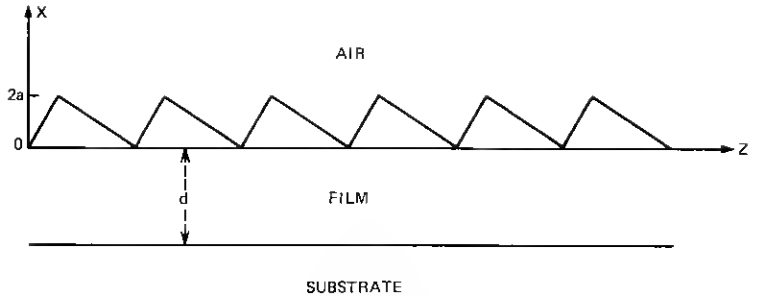

Fig. 2—The coordinate system in relation to the grating and the film.

agree well (in cases where agreement is to be expected) with the results of the exact grating theory. However, our present theory does not provide correct answers for the amplitudes of scattered waves inside the thin film that coincide with another guided mode. In this case, a "resonance" occurs and the results become meaningless. Coupling among guided modes thus cannot be handled by this theory and must be treated differently, as will be described later.

II. MATHEMATICAL FORMULATION OF THE PROBLEM

We use the following representation for the electric field[1] of the structure shown in Fig. 2:

$$E_y = \exp(-i\beta z) \sum_{m=-\infty}^{\infty} C_m \exp(-i\rho_m x) \exp\left(i\frac{2\pi}{D}mz\right) \quad \text{for } x \geqq 2a \quad (9)$$

$$E_y = \exp(-i\beta z) \sum_{n,m=-\infty}^{\infty} B_{nm} \exp[(i\pi/b)\, nx] \exp\left(i\frac{2\pi}{D}mz\right) \quad \text{for } 0 \leqq x \leqq 2a \quad (10)$$

$$E_y = \exp(-i\beta z) \sum_{m=-\infty}^{\infty} \{A_m^{(+)} \exp(-i\kappa_m x) + A_m^{(-)} \exp(i\kappa_m x)\} \exp\left(i\frac{2\pi}{D}mz\right) \quad \text{for } 0 \geqq x \geqq -d \quad (11)$$

$$E_y = \exp(-i\beta z) \sum_{m=-\infty}^{\infty} D_m \exp(i\sigma_m x) \exp\left(i\frac{2\pi}{D}mz\right) \quad \text{for } x \leqq -d. \quad (12)$$

We define

$$\beta_m = \beta - \frac{2\pi}{D}m \quad (13)$$

and express the parameters appearing in (9) through (12) as follows:

$$\rho_m^2 = n_2^2 k^2 - \beta_m^2 \tag{14}$$

$$\kappa_m^2 = n_1^2 k^2 - \beta_m^2 \tag{15}$$

$$\sigma_m^2 = n_3^2 k^2 - \beta_m^2. \tag{16}$$

The parameter b appearing in (10) is an arbitrary constant that should be larger than a. For our numerical evaluations we have used $b = a\sqrt{2}$. Equations (9), (11), and (12) are solutions of the wave equation but (10) is not. We solve our problem by substituting (10) into the wave equation, obtaining a set of equations for the determination of B_{nm}. However, these equations do not determine B_{nm} completely; in addition, we must satisfy boundary conditions by requiring that E_y and dE_y/dx remain continuous at $x = 2a$, $x = 0$, and $x = -d$. All these conditions lead to the following set of equation systems

$$\sum_{n',m'=-\infty}^{\infty} \left\{ N_{n'-n,m'-m} - \left[\left(\frac{\pi n'}{b} \right)^2 + \beta_{m'}^2 \right] M_{n,n'} \delta_{m,m'} \right\} B_{n',m'} = 0 \tag{17}$$

$$\sum_{n=-\infty}^{\infty} \left(\rho_m + \frac{\pi}{b} n \right) B_{nm} \exp\left(i \frac{2\pi}{b} na \right) = 0 \tag{18}$$

$$\sum_{n=-\infty}^{\infty} \left[\left(1 - \frac{\pi}{\kappa_m b} n \right) - \frac{\kappa_m - \sigma_m}{\kappa_m + \sigma_m} \exp\left(-2i\kappa_m d\right) \left(1 + \frac{\pi}{\kappa_m b} n \right) \right] B_{nm} = 0 \quad \text{for } m \neq 0. \tag{19}$$

If we remove the restriction $m \neq 0$ from (19), the combined equation system (17) through (19) would represent the exact formulation of our problem. However, since this would force us to solve the determinantal eigenvalue equation for complex β, we exclude the equation with $m = 0$ from (19) and add instead the following inhomogeneous equation to our set

$$\sum_{n=-\infty}^{\infty} \left[\left(1 - \frac{\pi}{\kappa_0 b} n \right) + \frac{\kappa_0 - \sigma_0}{\kappa_0 + \sigma_0} \exp\left(-2i\kappa_0 d\right) \left(1 + \frac{\pi}{\kappa_0 b} n \right) \right] B_{no} = 4A_0^{(+)}. \tag{20}$$

The equation system (17) stems from the substitution of (10) into the wave equation. The coefficients $M_{n,n'}$ and $N_{n'-n,m'-m}$ are defined in Ref. 1. Equations (18), (19), and (20) result from the boundary conditions. In fact, the left-most term in parenthesis in (20) as well as the term with the exponential function are each individually equal to $2A_0^{(+)}$. Equation

(20) is (twice) the arithmetic mean of these two equations and (19) (with $A_m^{(+)}$ instead of $A_0^{(+)}$) is their difference. We took the arithmetic mean of two equations, each expressing the relation between $A_0^{(+)}$ and B_{no}, to improve the accuracy of the approximation. The difference must, of course, be taken to eliminate $A_m^{(+)}$ from the exact equation system.

Equations (17) through (20) allow us to express B_{nm} in terms of $A_0^{(+)}$. For purposes of normalization, we express the amplitude coefficient $A_0^{(+)}$ in terms of the power P carried by the guided mode,

$$A_0^{(+)} = \left[\frac{\omega \mu_0 P}{\beta \left(d_{\text{eff}} + \frac{1}{\gamma_0} + \frac{1}{\delta_0} \right)} \right]^{1/2} \tag{21}$$

Finally, we need the amplitude coefficients of the scattered waves which may be expressed in terms of B_{nm} as follows,

$$C_m = \sum_{n=-\infty}^{\infty} B_{nm} \exp i \left(\rho_m + \frac{\pi}{b} n \right) 2a \tag{22}$$

and

$$D_m \exp(-i\sigma_m d) = \sum_{n=-\infty}^{\infty} \frac{\kappa_m(\kappa_m \cos \kappa_m d + i\sigma_m \sin \kappa_m d) - \frac{\pi}{b} n(\sigma_m \cos \kappa_m d + i\kappa_m \sin \kappa_m d) B_{nm}}{\kappa_m^2 - \sigma_m^2} \tag{23}$$

Knowing the amplitudes of all scattered waves, we can calculate the power that is carried away from the thin-film waveguide. We use the partial power attenuation coefficients

$$2\alpha_{2m} = \frac{\rho_m |C_m|^2}{2\omega \mu_0 P} \tag{24}$$

and

$$2\alpha_{3m} = \frac{\sigma_m |D_m|^2}{2\omega \mu_0 P} \tag{25}$$

and obtain the total power attenuation coefficient as the sum

$$2\alpha = \sum_m (2\alpha_{2m} + 2\alpha_{3m}), \tag{26}$$

where the summation extends over all real, propagating waves.

III. COUPLING COEFFICIENT BETWEEN GUIDED MODES

We are interested in finding the coupling coefficient for power transfer from the incident guided wave to its backward traveling counterpart. This is an important design parameter for distributed feedback lasers. The exact solution of our problem would give us this coefficient because we would know the amplitude coefficients of all the waves whether guided or not. Our approximate procedure fails if a principal grating lobe scatters power into the direction corresponding to another guided mode. For this reason, we use a different approach. If we want to couple the incident guided mode to the backward traveling mode via the first grating order, we need a grating period that is given by the formula,[5]

$$D = \frac{\pi}{\beta}. \tag{26}$$

A grating with such a short period does not scatter power out of the thin-film guide. We only need to know the amount of power scattered per unit length into the opposite direction. If the amplitude coefficient of this backward scattered wave is $A_1^{(-)}$, the coupling coefficient is defined as[6]

$$R = \frac{\kappa_0}{2\beta(d_{\text{eff}} + (1/\gamma_0) + (1/\delta_0))} \frac{A_1^{(-)}}{A_0^{(+)}}. \tag{27}$$

To first order of perturbation theory, we obtain from (27)

$$R = \frac{\kappa_0^2}{2\beta(d_{\text{eff}} + (1/\gamma_0) + (1/\delta_0))} a_1. \tag{28}$$

The factor a_1 is the Fourier coefficient of the spatial frequency component $2\pi/D$ of the grating function. For our triangular grating shape, we have

$$a_1 = \frac{2aD^2}{\pi^2(D - D_1)D_1} \sin \pi \frac{D_1}{D}. \tag{29}$$

We have stated the result of perturbation theory only for comparison purposes. We evaluate the coupling coefficient from (27) by calculating $A_1^{(-)}$ with the help of the exact grating theory developed in Ref. 1.

The simple, exact grating theory can be used to approximate waveguide losses by assuming that all waves that are scattered at the grating penetrate through the thin-film boundaries without any further reflection. We shall see that this assumption yields good results if the grating is on the side of the film with the greater index difference (the air side). For gratings on the substrate side, reflections from the opposite film boundary are important and the simple-minded approach yields unsatisfactory results. However, it is interesting to compare the results of the approximate theory presented here with loss calculations based

on the simple grating, since such a comparison can tell us when we can use the results of the simple grating theory directly and when we need the more sophisticated (if approximate) approach presented in this paper. A comparison of the two theories is also useful to give us confidence in the results of the approximate theory.

The partial waveguide losses can be computed from the simple grating theory by using (24) unchanged (except for the fact that the simple grating theory of Ref. 1 is now used to compute C_m) and by replacing D_m in (25) with A_m obtained from (16) of Ref. 1.

A discussion of the number of terms used in the series expansion of the field was given in Ref. 1.

IV. DISCUSSION OF RESULTS

Careful comparison of the results of our present theory with the perturbation theory[7] shows perfect agreement for small values of the grating depth $2a$. It is, of course, necessary to replace the amplitude of the sinusoidal grating (designated as σ in Ref. 7) with the Fourier amplitudes coefficient (29).

To show the difference of the scattering losses that result from using the present waveguide theory and to compare it to the simple grating theory, we have drawn in Fig. 3 the partial scattering loss of the first grating lobe for a grating with vanishingly small depth $2a$. The curves in this and subsequent figures are labeled accordingly. We normalize the loss coefficient by multiplying it with λ^3/a^2 to make it dimensionless and to reduce its dependence on a. To first order of perturbation theory the normalized attenuation coefficient should be independent of a.

The independent variable on the horizontal axis of all our figures is the scattering angle $\phi = 90 - \theta_{13}$ [see eq. (1)] of the first-order beam ($m = 1$), the wave corresponding to this angle escapes into the medium with the higher refractive index n_3. The angle ϕ is varied by varying the grating period D.

This practice of using the scattering angle of the substrate beam as the independent variable and defining it with respect to the direction normal to the film surface is taken from Ref. 7. Figure 3 and all subsequent figures use $n_1 = 1.59$, $n_2 = 1.0$, and $n_3 = 1.458$ (in some later figures, n_2 and n_3 will be interchanged). Furthermore, we use $d = d_{\text{eff}} = 0.571$; this choice was made to compare waveguides having the same effective width. Figure 3 applies to a symmetrical grating with $D_1/D = 0.5$. It is apparent how very similar the results of the two approaches are. The air beam disappears at an angle of 43.3°, because we have labeled all beams with the angle of the beam in the substrate and the angle of the air beam is related to the angle in the substrate by Snell's law.

A departure from the results obtained using the waveguide theory and the result calculated from the simple grating theory is discernible only

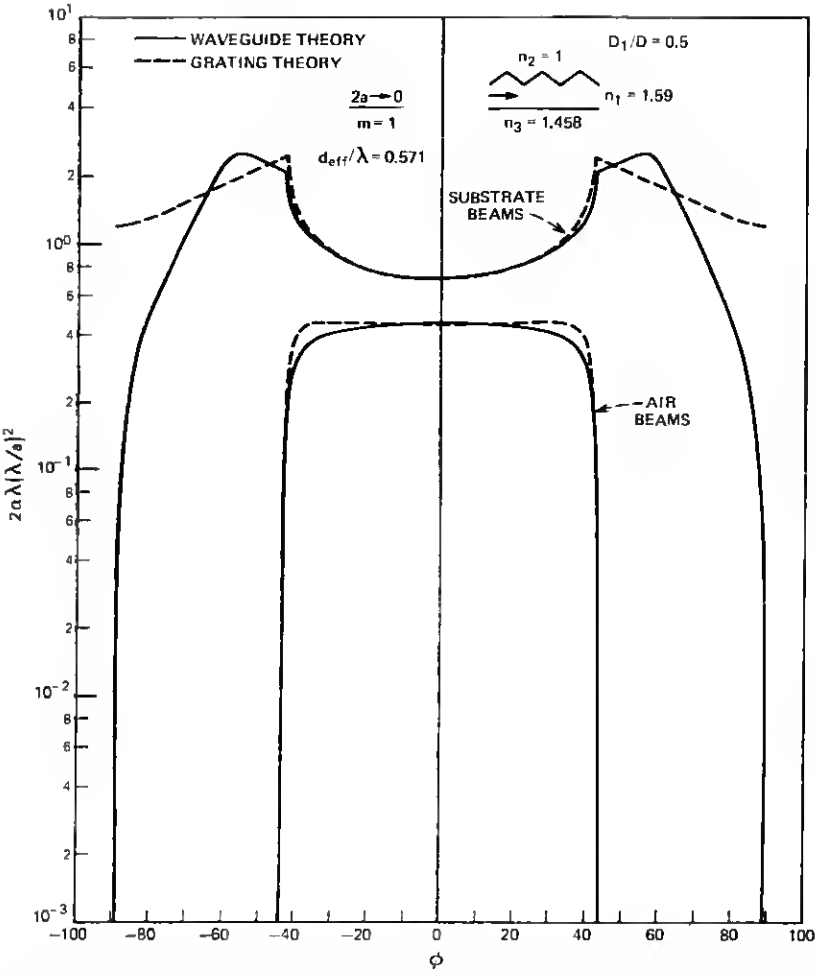

Fig. 3—Comparison of the waveguide grating theory with the simple grating theory for a symmetrical grating of vanishing depth ($2a/\lambda \to 0$). Shown is the normalized scattering loss coefficient of the first-order substrate beam. Film index $n_1 = 1.59$, air index $n_2 = 1$, substrate index $n_3 = 1.458$.

at beam angles that correspond to beams that nearly graze the surface. At these angles, reflection from the film-substrate interface becomes noticeable and indicates the difference in the solid and dotted curves. In particular, we see that the substrate beam, expressed by the solid line, vanishes at $\phi = \pm 90°$, whereas the dotted line remains at a finite value. This difference is caused by the fact that the substrate beam goes over into a guided mode in the waveguide case, but in the simple grating, where no guided modes exist, the scattering angle in the film can become still larger so that there is no discontinuity at the point where the actual

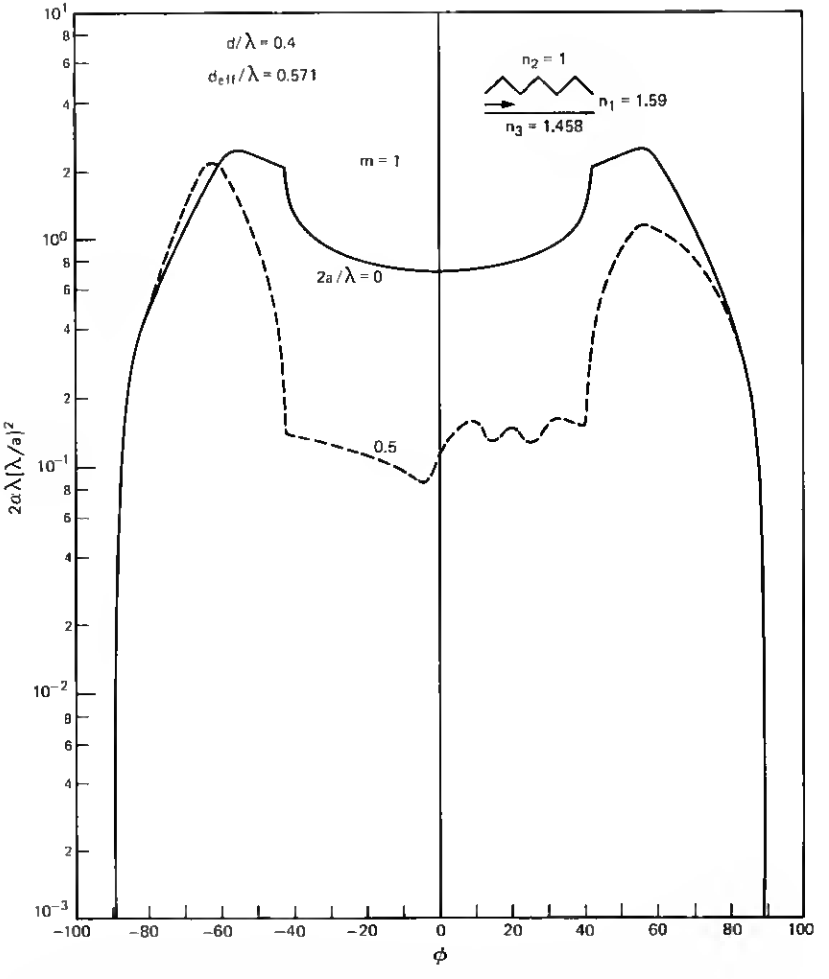

Fig. 4—Substrate beams: comparison of perturbation theory ($2a/\lambda \to 0$) and thick grating waveguide theory ($2a/\lambda = 0.5$) for a symmetrical grating on the air side of the film. The first-order substrate beam loss is shown.

substrate beam vanishes. However, the angle of the simple grating response has been adjusted by Snell's law to correspond not to the film but to the substrate angle, even though reflection at this interface does not exist in case of the simple grating.

Figure 4 provides a comparison between perturbation theory ($2a/\lambda \to 0$) and the first-order grating response for a grating on a thin-film waveguide with thickness $2a/\lambda = 0.5$. We have used a film thickness of $d/\lambda = 0.4$, but the thick grating increases the effective film thickness to $d_{eff}/\lambda = 0.571$. To have a meaningful comparison, we have used this film thickness also for the case $a \to 0$. Figure 4 shows clearly that per-

turbation theory overestimates the scattering losses of thick gratings. However, for ϕ near $\pm 90°$, the agreement between perturbation theory and the more precise theory is still remarkably close. This seems to be a general tendency which we shall encounter again. Figure 4 holds for the substrate beam while Fig. 5 shows a comparison between perturbation theory and the more precise theory for the air beam. Figure 6 applies to the same case, i.e., a symmetrical grating on the air side of the film, and shows the total scattering loss (power carried away by all grating orders in both media) as the solid line and compares it with the power carried away by the first-order grating response in the substrate indicated by the dotted line. The difference between the total amount of scattered power and the power in the first-order substrate beam is made

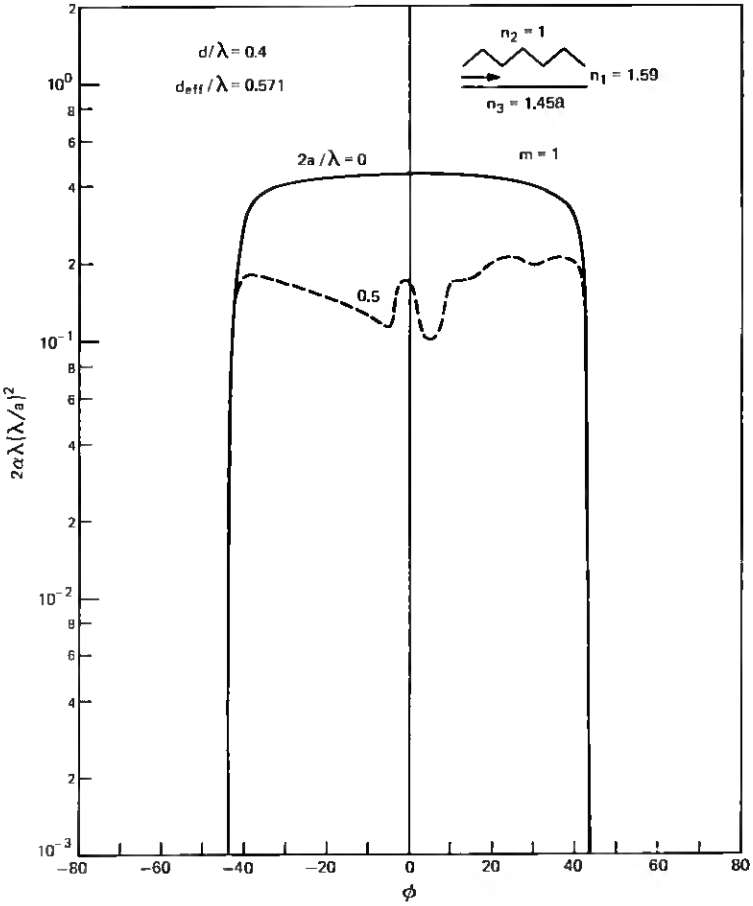

Fig. 5—Air beams: comparison of first-order perturbation theory ($2a/\lambda = 0$) with thick grating theory ($2a/\lambda = 0.5$) for the air beam with grating on air-film interface.

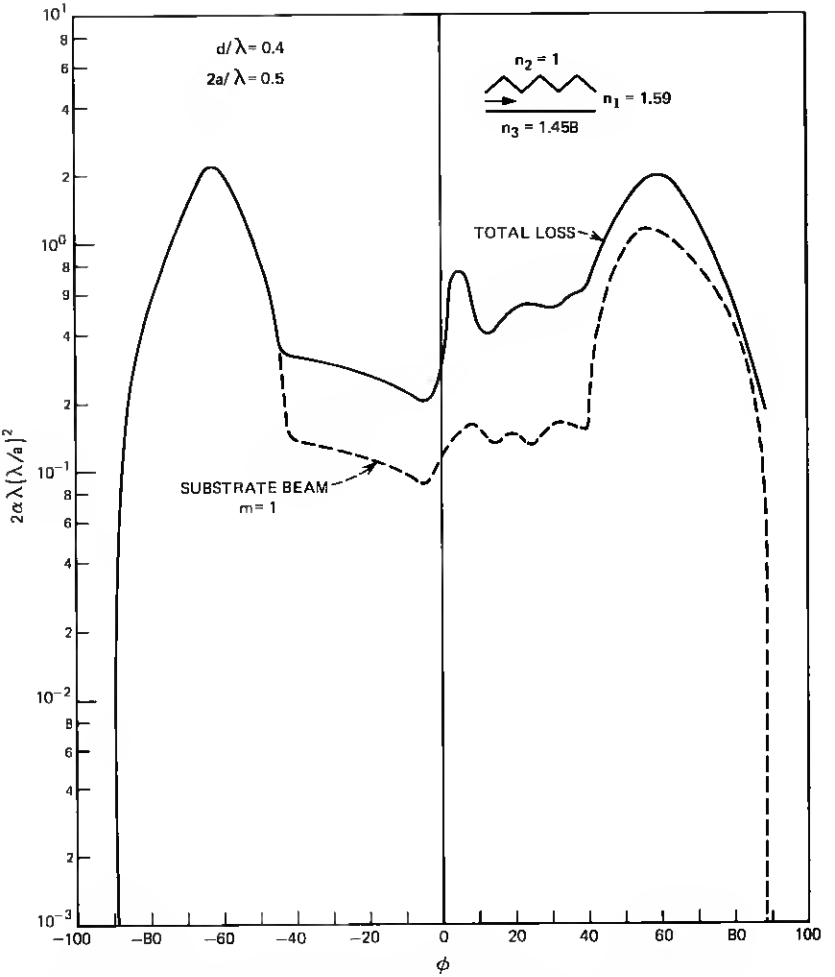

Fig. 6—The total loss is compared to the loss caused by the first-order substrate beam for $2a/\lambda = 0.5$ and a symmetrical grating on the air-film interface.

up partly by the power carried by the first-order air beam and partly by all the other grating orders. As the angle ϕ increases, more and more grating lobes appear. Rather than show each grating order separately we have added them all and have presented the total loss. The curve representing the total loss does not go to zero at $\phi = 90°$, because the grating responses of higher order do not vanish as the first-order substrate beam disappears inside of the thin film.

Fig. 7 shows the scattering losses of an asymmetric grating on the air side of the thin film with $D_1/D = 0$. We have included the total scattering loss as the topmost solid line, the first-order substrate beam as the dotted

line, and the first-order air beam as the lowest solid line. The most conspicuous aspect of this figure is the fact that so much more power is carried by the first-order substrate beam compared to the first-order air beam. The grating asymmetry is responsible for preferential scattering into the substrate. Comparison of Figs. 4 and 5 shows that the symmetrical grating scatters roughly equal amounts of power into air and substrate in the angular range where both beams exist simultaneously. Fig. 7 shows that a relatively small amount of power is scattered into higher-order grating modes, because the curve for the first-order substrate beam does not lie far below the total loss curve.

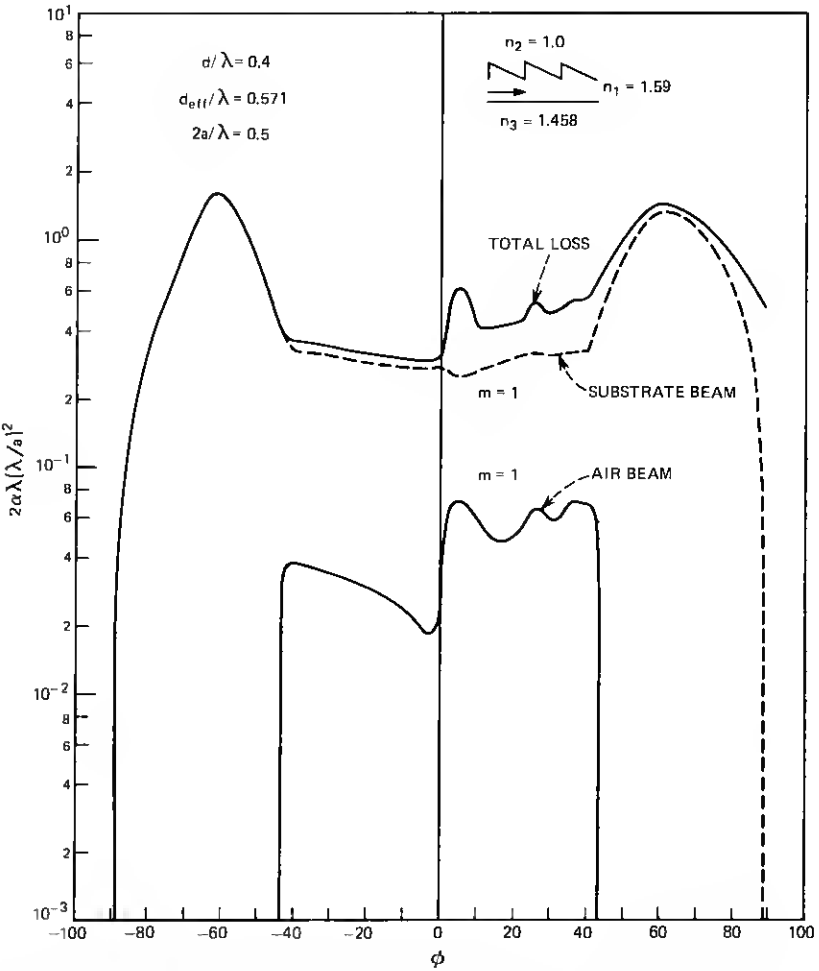

Fig. 7—Total loss, first-order substrate beam, and first-order air beam loss for an asymmetrical grating with $D_1/D = 0$ and $2a/\lambda = 0.5$.

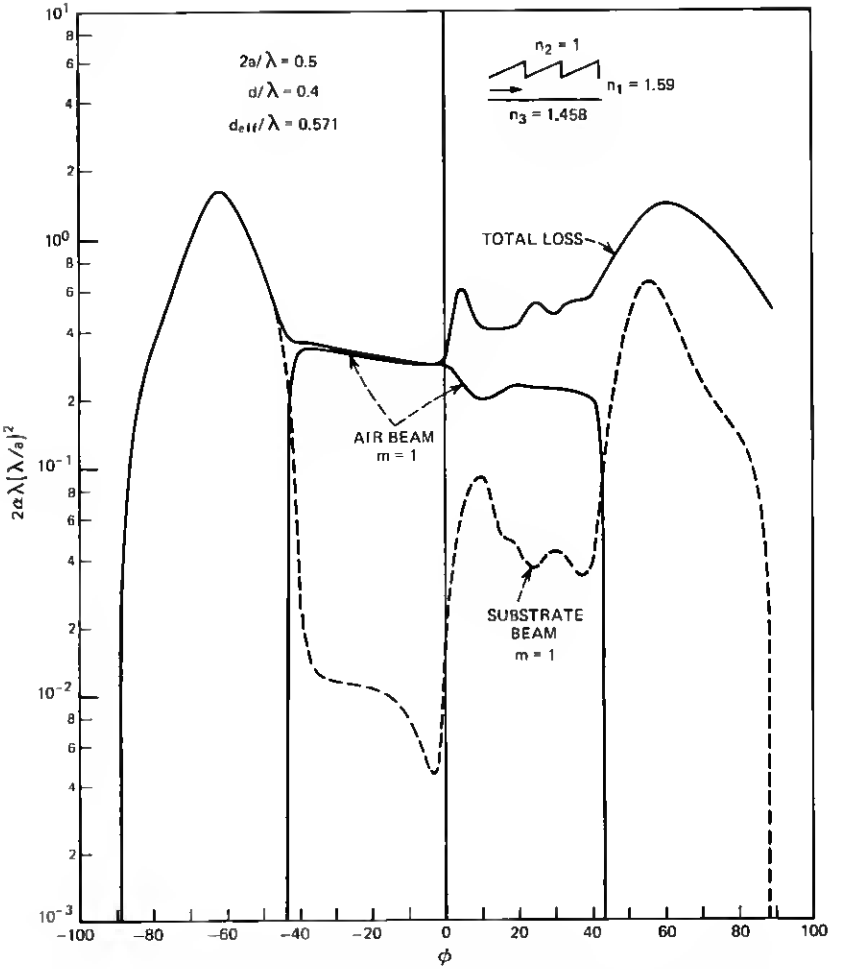

Fig. 8—Same comparison as in Fig. 7 for an asymmetrical grating with $D_1/D = 1$.

Figure 8 applies to a grating with the opposite asymmetry, $D_1/D = 1$. The total loss is the same as in Fig. 7 but the roles of substrate and air beams have been interchanged in the range $-43° < \phi < 43°$. For angles below this range, the substrate beam is identical to the corresponding beam for the grating with the opposite symmetry. For $\phi > 43°$, the substrate beam carries again significantly higher power than inside the range $-43° < \phi < 43°$ but higher-order modes now carry far more power at angles $\phi > 43°$ than in Fig. 7. An explanation of the influence of the grating shape in terms of geometrical optics is given in Ref. 1.

We have compared the results of the waveguide grating theory with the simple grating theory in Fig. 3 for the case of very thin gratings.

Figures 9 and 10 show such a comparison for a thick, asymmetric grating with $2a/\lambda = 0.5$ and $D_1/D = 1$. We see that we can obtain most of the scattering information from the simple grating theory. The two curves depart significantly only near the ends of the angular range of the substrate beam.

So far we have considered only gratings on the air side of the thin film. The next six figures apply to gratings on the substrate side of the film. We obtain these results from our theory simply by interchanging the roles of n_2 and n_3, with the values $n_1 = 1.59$, $n_2 = 1.458$, and $n_3 = 1.0$. For a deep grating with $2a/\lambda = 0.5$ and $d/\lambda = 0.4$, we now obtain a very

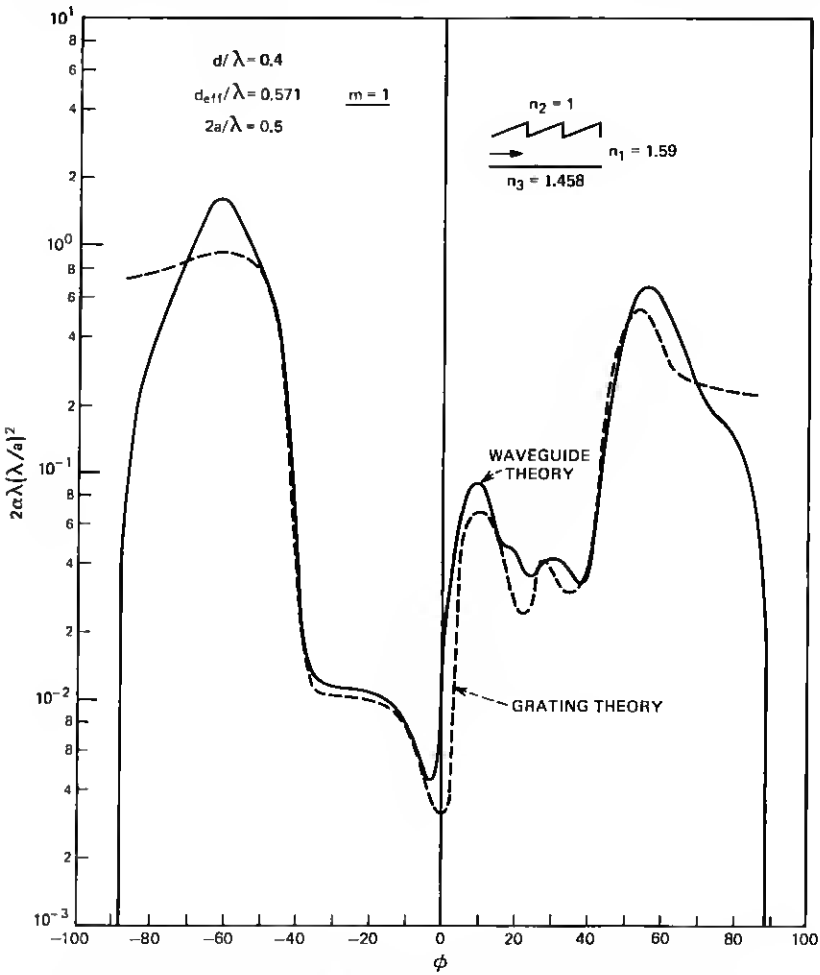

Fig. 9—Substrate beams: comparison of the grating guide theory with the simple grating theory for an asymmetrical grating with $D_1/D = 1$ for $2a/\lambda = 0.5$. The partial loss coefficient for the first-order substrate beam is shown.

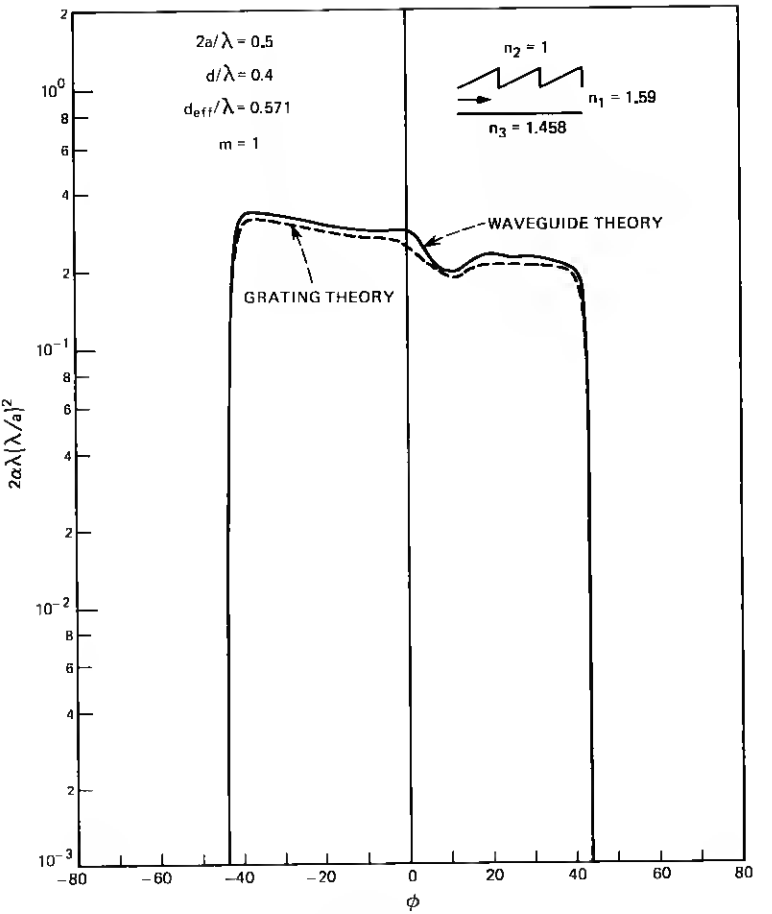

Fig. 10—Same as Fig. 9 for first-order air beams.

slightly different effective film thickness of $d_{\text{eff}}/\lambda = 0.569$. Figure 11 shows a comparison of perturbation theory ($2a/\lambda \to 0$) and thick grating theory for $2a/\lambda = 0.5$ for the first-order substrate beam for a symmetrical grating with $D_1/D = 0.5$. This figure should be compared with Fig. 4, because both cases are similar with the only difference being that the grating is now on the opposite side of the thin film. The thick grating theory is now in much closer agreement with perturbation theory, but both theories show a markedly different behaviour from the curves in Fig. 4, since there is obviously far more interference between the direct beam and the component that is reflected only once at the air-film interface. The deeper nulls discernible in the thick grating theory (dotted lines in Fig. 11) are caused by the fact that a slight shift has occurred that places the regions of destructive interference at angles where total in-

ternal reflection occurs at the air-film interface. Figure 12 shows a similar comparison for the first-order air beam for the same grating geometry. This figure should be compared with Fig. 5. Figure 12 is quite similar in shape to Fig. 5, but the curves are much lower, showing that air beam scattering is weaker if the grating is on the substrate side of the film. There are no pronounced interference effects, because the reflection from the film-substrate interface is much weaker. The dotted line in Fig. 12 labeled grating theory was computed with the help of the simple grating theory and shows remarkably close agreement with the grating guide theory.

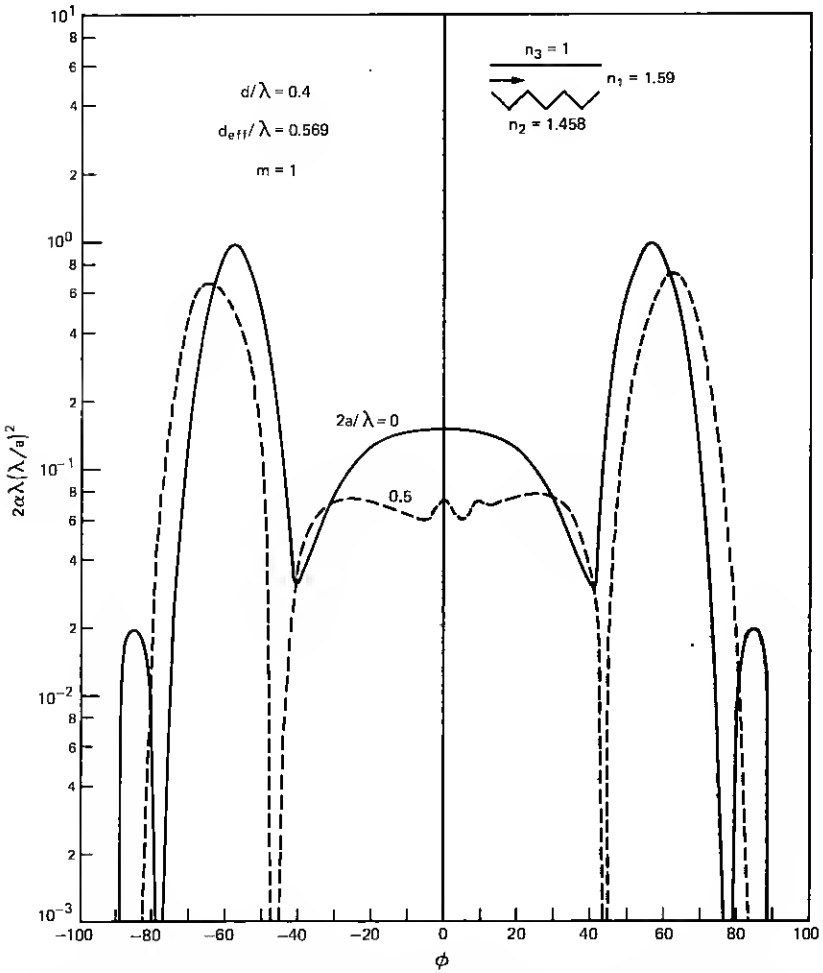

Fig. 11—Substrate beams: grating on film-substrate interface. Comparison between perturbation theory and thick waveguide grating theory ($2\alpha/\lambda = 0.5$) for a symmetrical grating, $D_1/D = 0.5$ for first-order substrate beams. Note the deep interference nulls.

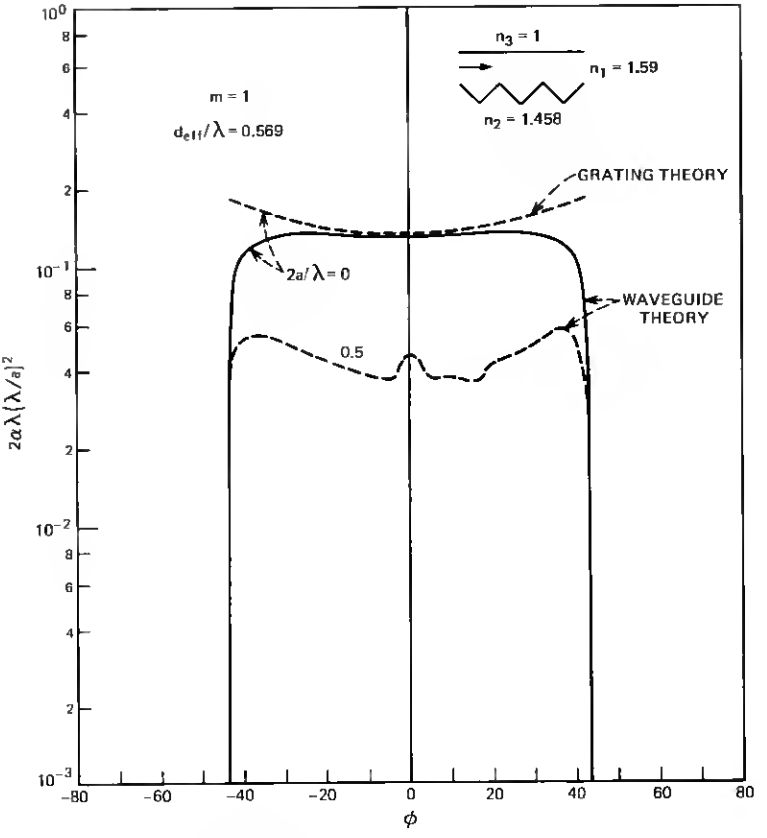

Fig. 12—Same as Fig. 11 showing the first-order air beams.

Figure 13 compares the total loss to the loss associated with power carried away by the first-order substrate beam for a thick grating with $2a/\lambda = 0.5$.

Figure 14 compares the theory of the simple grating with the waveguide grating theory for the first-order substrate beam for a thin grating ($2a/\lambda \rightarrow 0$) at the film-substrate interface. We see that the simple grating theory does not always suffice to predict the performance of a thin-film waveguide with a diffraction grating. The simple grating theory predicts the average loss correctly, but fails completely to account for interference effects. This figure should be compared with Fig. 3. The comparison shows that the simple theory is quite useful as long as interference effects between a direct and a reflected beam can be neglected, as in the case of the grating on the film-air interface (Fig. 3). For a grating on the film-substrate interface (Fig. 14), the simple grating theory is not applicable to the waveguide case. Figure 15 shows the comparison of the

two theories for a thick grating with $2a/\lambda = 0.5$ for the first-order substrate beam, whereas Fig. 16 compares the corresponding first-order beam in the air space. Just as in Fig. 12, the simple grating theory gives a good description of scattering for the air beam even if the grating is thick and is located on the film-substrate interface.

The last figure, Fig. 17, shows the normalized coupling coefficient R (multiplied by λ^2/a) as a function of the normalized grating thickness $2a/\lambda$ for gratings on the film-air interface (solid lines) and on the film-substrate interface (dotted lines) for symmetric ($D_1/D = 0.5$) and asymmetric gratings ($D_1/D = 0$ and 1). The two extreme cases of

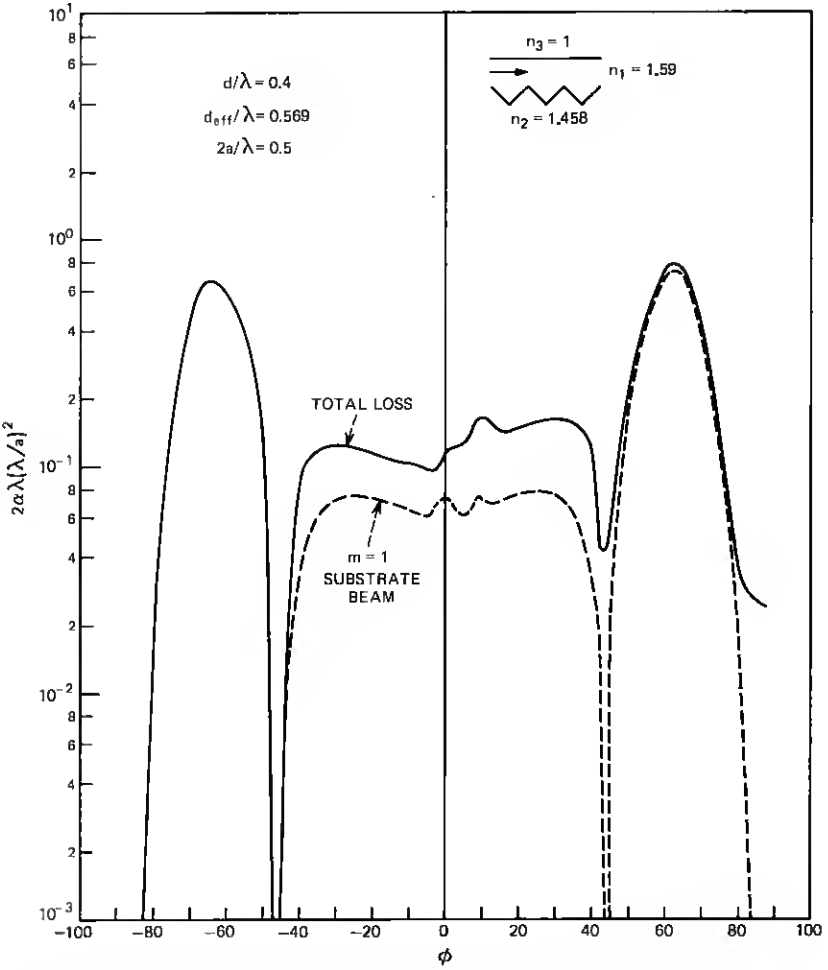

Fig. 13—Comparison of total loss and partial first-order substrate beam loss for a symmetrical grating on the film-substrate interface.

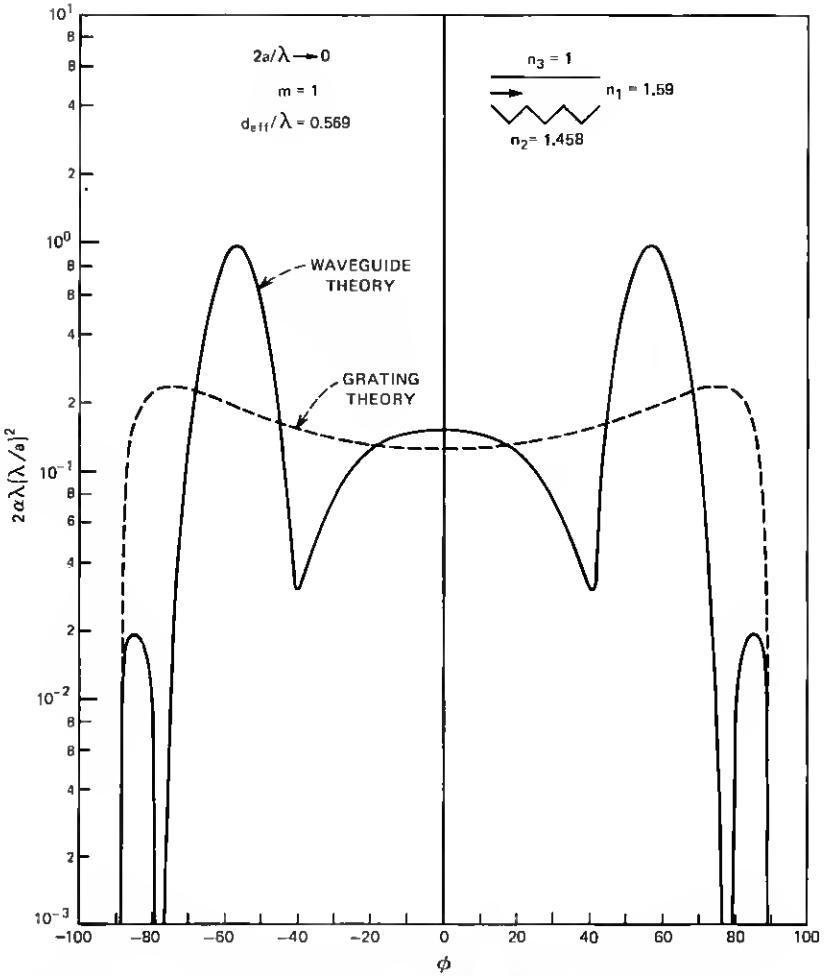

Fig. 14—Substrate beams: comparison of the waveguide grating theory and the simple grating theory for a thin grating ($2a/\lambda \to 0$) on the film-substrate interface.

asymmetry give exactly the same results. At $2a/\lambda = 0$ the curves agree, of course, with the perturbation theory (28). The most remarkable fact about the curves of Fig. 17 is their slight departure from the prediction of perturbation theory. Corresponding curves drawn from perturbation theory would be straight horizontal lines coinciding with our curves at $2a/\lambda = 0$. The exaggerated scale of the figure shows the downward slope for increasing grating thickness, but even for a grating whose thickness is equal to the vacuum wavelength of the wave, the results of the thick grating theory differ from perturbation theory by no more than 30%. This result is in agreement with the general trend that we observed in Fig. 4,

where we saw that the thick grating theory is in close agreement with perturbation theory near $\phi = -90°$. Coupling between a forward and backward traveling guided mode is an extreme case of backward substrate scattering, except that the beam does not escape into the substrate but is trapped in the film by total internal reflection. Figure 4 shows clearly how much perturbation tbeory and thick grating theory can differ at scattering angles that are more nearly normal to the film surface. Figure 17 thus shows that the perturbation formula (28) is remarkably accurate even for rather thick gratings whose thickness approaches the vacuum wavelength of the light wave. The curves in Fig. 17 were com-

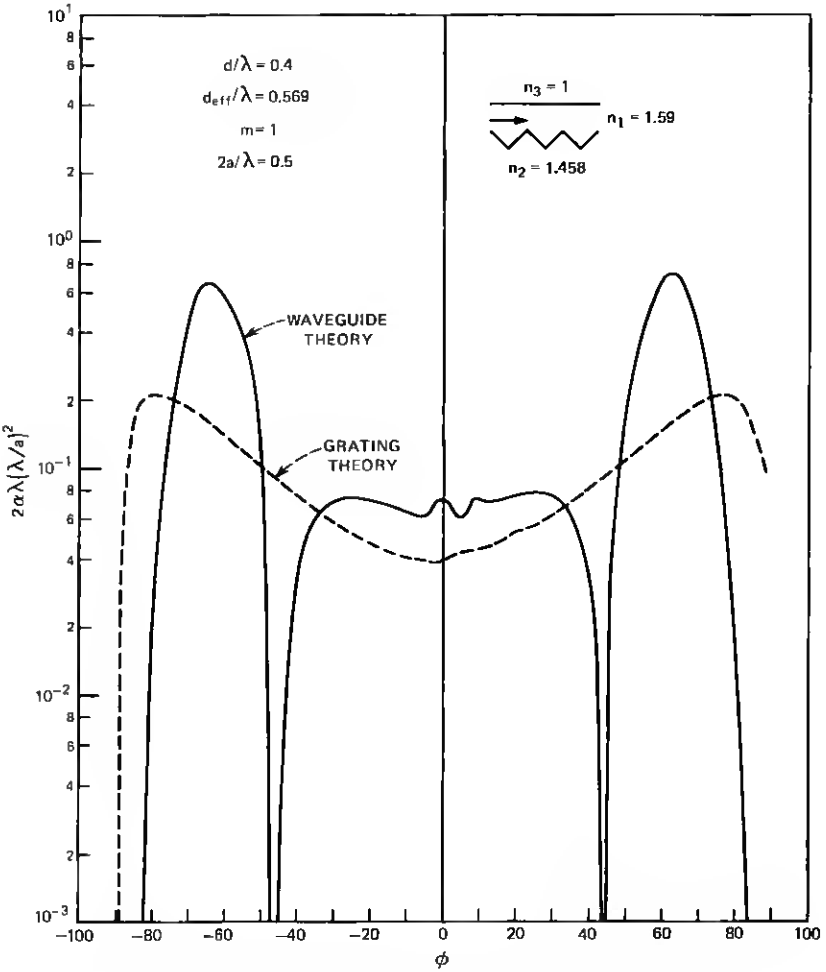

Fig. 15—Same as Fig. 14 for thick grating with $2a/\lambda = 0.5$.

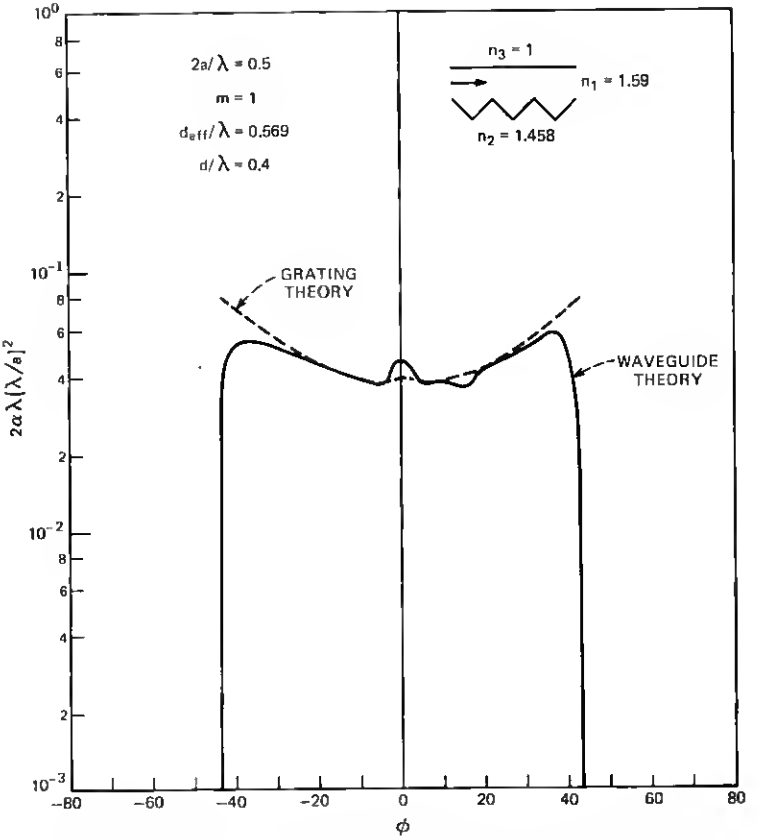

Fig. 16—Same as Fig. 15 showing the partial loss coefficients for first-order air beam scattering.

puted from (27), where the scattered wave amplitude $A_1^{(-)}$ is obtained from the simple grating theory.[1]

V. CONCLUSIONS

We have presented an approximate theory for scattering of power from a guided thin-film mode into the areas above and below the film by a thick diffraction grating deposited on one side. This theory has been compared with perturbation theory[7] and with the results of the exact, simple grating theory for a grating between two dielectric half spaces, and good agreement has been obtained in all cases where agreement can be expected. We are confident that our theory yields reasonable results for light scattering out of a thin film.

However, this theory does not give correct answers if applied to cou-

pling between two guided modes, even in the limit of very thin gratings where the correct answer is known from perturbation theory. This failure of the theory in the case of coupling among guided modes is understandable when we realize that a guided mode is at transverse resonance in the thin-film guide. The naive theory, that is based on the assumption that the mode amplitudes remain constant along the thin film, cannot account for a resonant situation where the power exchange may be complete and where mode coupling leads to new normal modes of the structure. On the other hand, it does not seem to hurt the calculation of the radiation loss coefficients if a minor grating lobe accidentally scatters power into the direction of a guided-film mode. Such "resonances" do occur, for example, over the angular range shown in Fig. 3

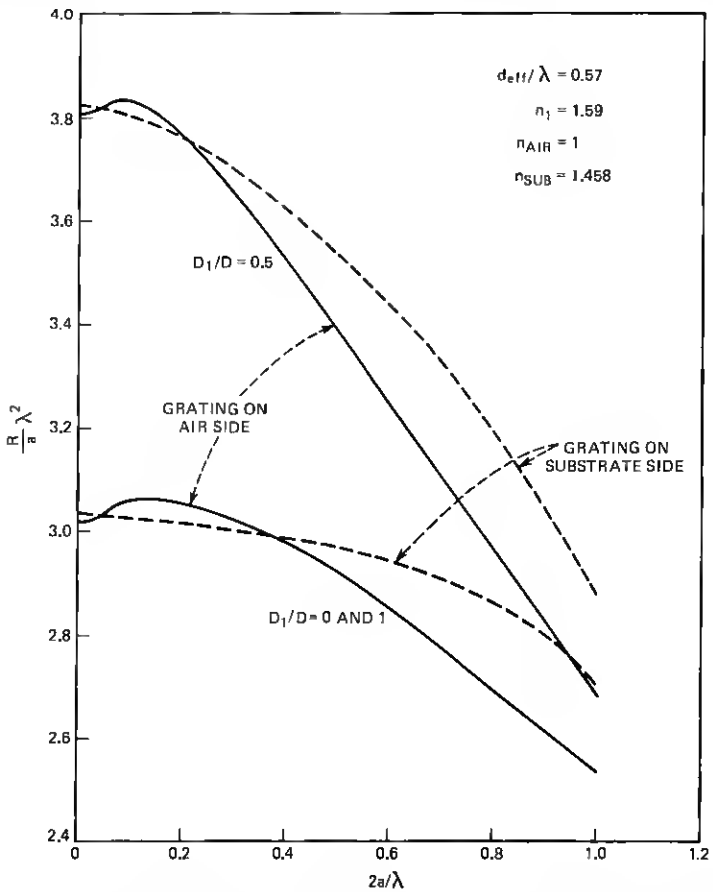

Fig. 17—Coupling coefficients between forward and backward guided mode. The solid lines hold for a grating on the film-air interface, the dotted lines describe a grating on the film-substrate interface. The curves for $D_1/D = 0$ and $D_1/D = 1$ are identical.

and the excellent agreement with perturbation theory and with the simple exact grating theory indicates that no difficulties have occurred.

Our theory has helped to clarify the areas where the simple grating theory[1] may be used to predict scattering losses even for film waveguides, but it has also shown that the simple grating theory does not help to predict waveguide losses if strong interference between a direct and a reflected beam may occur.[8]

Finally, we have used the simple grating theory to compute the coupling coefficient between two guided modes traveling in opposite directions. We found that perturbation theory holds approximately over a surprisingly wide range of grating thicknesses. Coupling between modes other than forward and backward modes could be treated very similarly.

Our approximate waveguide grating theory has the advantage of allowing direct calculations of power scattering without the need for a search routine for finding the complex roots of a large determinantal equation. It is, thus, a cheap and fast method for calculating the scattering properties of thick gratings on thin-film waveguides.

VI. ACKNOWLEDGMENT

The author acknowledges the contribution made to this paper by fruitful discussions with W. W. Rigrod.

REFERENCES

1. D. Marcuse, "Exact Theory of TE-Wave Scattering From Blazed Dielectric Gratings," B.S.T.J., *55*, No. 8 (October 1976) pp. 1295–1317.
2. T. Tamir, "Beam and Waveguide Couplers," in *Topics in Applied Physics*, Vol. 7 of *Integrated Optics*, New York: Springer Verlag, 1975, pp. 83–137.
3. M. Born and E. Wolf, *Principles of Optics*, Third ed., New York: Pergamon Press, 1965.
4. D. Marcuse, "Theory of Dielectric Optical Waveguides," New York: Academic Press, 1974, Eq. (1.2–12), p. 6.
5. H. Kogelnik and C. V. Shank, "Coupled Wave Theory of Stimulated Emission in Periodic Structures," J. Appl. Phys. *43*, No. 5 (May 1972), pp. 2327–2335.
6. Ref. 4, Eq. (4.3–33), p. 151.
7. W. W. Rigrod and D. Marcuse, "Radiation Loss Coefficients of Asymmetric Dielectric Waveguides with Shallow Sinusoidal Corrugations," IEEE J. Quant. Electron., *QE-12*, No. 11 (November 1976), pp. 673–685.
8. W. Streifer, R. D. Burnham, and D. R. Scifres, "Analysis of Grating-Coupled Radiation in GaAs: GaAlAs Lasers and Waveguides—II: Blazing Effects," IEEE J. Quant. Electron., *QE-12*, No. 8 (August 1976), pp. 494–499.